in-plane shielding components. Unfortunately, the present model cannot be applied to the perpendicular component σ_{33}, which is determined by factors more complex than the bond orders. It is apparent that the values of σ_{33} are consistent with the qualitative predictions of the ring current model[27], but a detailed analysis is deferred until a more extensive theory can be applied to a molecule of this size.

The results presented here for a fused aromatic molecule point toward an important method to assess the relative aromaticity of the individual bonds in a molecule. Contrary to other techniques,[9] which focus on the molecule as a whole, the measurement of ^{13}C shielding tensors in polycyclic aromatic compounds presents a premier tool for the analysis of the aromatic character of individual bonds in the molecule. The rules established here correlate the degree of aromaticity of the adjacent bonds with the ^{13}C measured shielding tensors in pyrene. Moreover, this rule holds for a large number of polycyclic aromatic compounds studied theoretically.[28]

The richness of the full tensor description of chemical shielding in pyrene stands in sharp contrast to the liquid results where all of the observed lines are within 7 ppm of one another, illustrating once more the power of modern NMR of solids.

Acknowledgment. This work was supported by the DOE under Grant DE-FG02-86ER13510 and by the NSF Grant CHE-8310109.

Registry No. Pyrene, 129-00-0.

(27) Haigh, C. H.; Mallion, R. B. *Prog. NMR Spectrosc.* **1980**, *13*, 303.

(28) Facelli, J. C.; Grant, D. M. *Theor. Chim. Acta*, in press.

Spin Coupling in Metalloporphyrin π-Cation Radicals

Brian S. Erler, William F. Scholz, Young Ja Lee,[1] W. Robert Scheidt,*[1] and Christopher A. Reed*

Contribution from the Departments of Chemistry, University of Southern California, Los Angeles, California 90089-1062, and University of Notre Dame, Notre Dame, Indiana 46556.
Received August 8, 1986

Abstract: The magnetic interactions between metal and ligand spins in metalloporphyrin π-cation radicals have been investigated as a function of d orbital type for synthetically accessible $S = {}^1/_2$ metals from the first transition series. Most instructive is the case of copper(II) where the presumably planar $[Cu(TMP^{\bullet})]^+$ (TMP$^{\bullet}$ = π-cation radical of tetramesitylporphyrinate) has an overall $S = 1$ state ($\mu_{eff} = 2.99\ \mu_B$). The ferromagnetic coupling of spins is rationalized as arising from the exchange interaction of unpaired electrons in orthogonal magnetic orbitals. By contrast, $[Cu(TPP^{\bullet})]^+$ has a ruffled porphyrin core in the solid state and is diamagnetic ($S = 0$). The antiferromagnetic coupling is rationalized in terms of overlap of the magnetic orbitals, i.e., bond formation with spin pairing in the bonding molecular orbital. The same principles seem to apply to the analogous systems of V(IV), Co(II), and low-spin Fe(III), where in each case the metal unpaired electron is in a different d orbital. Some reinterpretation of previous conclusions is required. The crystal and molecular structure of $[Cu(TPP^{\bullet})][SbCl_6]$ has been determined. The structure consists of $[Cu(TPP^{\bullet})]^+$ ions that interact in pairs in the crystalline lattice. Dimer formation is believed to be the cause of the exceptionally small dihedral angles between the peripheral phenyl rings and the porphinato core (average value 41.5°). This dimerization is also responsible for the unusual saddle-shaped core conformation. This conformation has also been observed in other π-cation radical species. The observed Cu-N bond distance of 1.988 (4) Å is typical of that for copper(II) and confirms the ring-oxidized nature of the compound. Crystal data: $a = 13.484$ (2) Å, $b = 13.924$ (3) Å, $c = 12.886$ (2) Å, $\alpha = 98.90$ (2)°, $\beta = 111.08$ (1)°, $\gamma = 106.97$ (2)°, triclinic, $P\bar{1}$, $Z = 2$, $CuN_4C_{44}H_{28}SbCl_6$. The ultimate simplicity and apparent generality of the spin-coupling theory provide one of the most accessible and heuristically useful entries to understanding the fundamental concepts of magnetic coupling phenomena.

In a recent paper on iron(III) porphyrin π-cation radical complexes[2] we proposed a theory to account for the notable difference in coupling of metal and ligand spins in $Fe(OClO_3)_2(TPP^{\bullet})$ and $[FeCl(TPP^{\bullet})]^+$ (TPP$^{\bullet}$ = π-cation radical of tetraphenylporphyrinate).[3] Spin coupling in the former is ferromagnetic. In the latter it is antiferromagnetic. The theory is based on the occupations and symmetries of the so-called magnetic orbitals, i.e., those orbitals on the metal and the ligand that contain an unpaired electron. The diversity of d orbital occupations and symmetries across the first transition series provides an excellent opportunity to probe the scope and generality of this theory. Metalloporphyrin π-cation radical complexes whose half-occupied d orbitals are strictly orthogonal to the porphyrin π-radical orbital are expected to show ferromagnetic coupling (like Hund's rule). Thus, the spin state of higher multiplicity will be lower in energy. For example, in a strictly planar environment of D_{4h} symmetry, $Cu^{II}(porph^{\bullet})$ would have orthogonal metal ($d_{x^2-y^2}$) and ligand (a_{1u} or a_{2u}) magnetic orbitals and be expected to show an $S = 1$ (i.e., triplet) ground state. On the other hand, complexes whose metal and ligand magnetic orbitals are not strictly forbidden by symmetry to overlap are expected to show *antiferro*magnetic coupling (or bond formation). The spin state of lower multiplicity will be lower in energy. For example, in a nonplanar environment of say C_{2v} symmetry, $Cu^{II}(porph^{\bullet})$ would be expected to have an $S = 0$ (i.e., singlet) ground state. Earlier[4] we noted the existence of the latter state in the diamagnetic crystalline solid $[Cu(TPP^{\bullet})][SbCl_6]$, and we now present evidence for the antithetic case in the mesityl analogue $[Cu(TMP^{\bullet})][SbCl_6]$. We also explore the syntheses and properties of π-cation radical complexes of V, Co, and Ni. Like copper, the vanadyl and cobalt cases provide $S = {}^1/_2$ metals, but the particular half-occupied d orbital is different in each case. These studies lead to a reinterpretation of certain published data and suggest there may be

(1) University of Notre Dame.

(2) Gans, P.; Buisson, G.; Duée, E.; Marchon, J.-C.; Erler, B. S.; Scholz, W. F.; Reed, C. A. *J. Am. Chem. Soc.* **1986**, *108*, 1223.

(3) Abbreviations used in this paper: TPP = tetraphenylporphyrinate, OEP = octaethylporphyrinate, TMP = tetramesitylporphyrinate, and SCE = saturated calomel electrode.

(4) Scholz, W. R.; Reed, C. A.; Lee, Y. J.; Scheidt, W. R.; Lang, G. *J. Am. Chem. Soc.* **1982**, *104*, 6791-6793.

0002-7863/87/1509-2644$01.50/0

a wide generality to the present view of the spin-coupling mechanisms.

Experimental Section

General. UV-vis spectra were recorded on a Shimadzu UV-260 spectrophotometer and IR spectra on a Perkin-Elmer 281. H_2OEP was purchased from Aldrich. H_2TPP was synthesized by the usual method,[5] and chlorin impurity was removed by DDQ oxidation[6] followed by chromatography with $CHCl_3$ on neutral alumina. H_2TMP was prepared similarly by literature methods.[7] Solvents were purified by standard methods[8] (sulfuric acid washed, base washed, dried, distilled from CaH_2 or sodium/benzophenone) and stored over molecular sieves. Reactions were carried out under nitrogen (H_2O < 10 ppm) in Schlenkware with Teflon stopcocks by using canular techniques. Organic radical cation salts were prepared as previously described.[2] **Caution**: perchlorate salts can detonate spontaneously. Although no explosions were encountered in this work, precautions are warranted. Reactions involving ClO_4^- were always run on a small scale, and materials were not stored for long periods. KBr disks for IR spectroscopy were prepared in an inert atmosphere glove box (H_2O < 1 ppm).

Syntheses. **[Cu(TPP•)][SbCl$_6$]·0.5CH$_2$Cl$_2$.** Cu(TPP) (0.10 g, 0.15 mmol) and phenoxathiinylium hexachloroantimonate (0.081 g, 0.15 mmol) were stirred in dichloromethane (20 mL) for 15 min. The green solution was filtered, and crystallization was induced by careful layering with heptane. Dark-purple crystals were collected and washed with heptane: 0.11 g, 70%; UV λ_{max} (CH_2Cl_2) 630, 575, 437 sh, 408 Soret nm; IR (KBr) 1295 vs (TPP•) cm^{-1}. Anal. Calcd for $C_{44.5}H_{29}CuCl_7N_4Sb$: C, 50.75; H, 2.77; N, 5.31; Cl, 23.56. Found: C, 50.82; H, 2.47; N, 5.29; Cl, 23.22. The perchlorate salt was prepared in a similar manner and crystallized as a dichloromethane solvate. Anal. Calcd for $C_{49}H_{38}CuCl_3N_4O_4$: C, 64.70; H, 4.18; N, 6.11. Found: C, 64.16; H, 4.31; N, 6.23.

[Cu(TMP•)][SbCl$_6$]·C$_6$H$_5$F. Cu(TMP) (0.100 g, 0.12 mmol) and phenoxathiinylium hexachloroantimonate (0.063 g, 0.12 mmol) were stirred in fluorobenzene (20 mL) for 2 days. The resulting dark-green precipitate was washed with fluorobenzene and dried under vacuum: 0.10 g, 65%; UV λ_{max} (CH_2Cl_2) 656, 596, 407 Soret nm; IR (KBr) 1280 vs (TMP•), 350 vs (Sb–Cl) cm^{-1}; χ_{dia} -1059×10^{-6} cgs. Anal. Calcd for $C_{62}H_{57}CuCl_6FN_4Sb$: C, 58.40; H, 4.15; N, 4.39; Cl, 16.68. Found: C, 58.15; H, 4.44; N, 4.31; Cl, 16.13.

[VO(TPP•)][SbCl$_6$]. VO(TPP) (0.100 g, 0.15 mmol) was dissolved in dichloromethane (20 mL), giving a bright-red solution. Phenoxathiinylium hexachloroantimonate (0.080 g, 0.15 mmol) was added and the green solution stirred overnight. The green precipitate was collected by filtration and washed with dichloromethane: 0.134 g, 82%; UV λ_{max} (CH_2Cl_2) 415 Soret, 600, 660 nm; IR (KBr) 1280 vs (TPP•), 345 vs (Sb–Cl) cm^{-1}; χ_{dia} -865×10^{-6} cgs. Anal. Calcd for $C_{44}H_{28}N_4OCl_6VSb$: C, 52.11; H, 2.78; N, 5.52; Cl, 20.98. Found: C, 51.90; H, 3.06; N, 5.30; Cl, 20.91. The corresponding perchlorate complex was characterized spectroscopically and found to be essentially identical. The lack of splitting of the ClO_4^- modes at 1080 and 615 cm^{-1} and ν(Sb–Cl) above in the IR spectrum suggest an ionic formulation.

[Ni(OEP•)][SbCl$_6$]. Ni(OEP) (0.100 g, 0.17 mmol) and phenoxathiinylium hexachloroantimonate (0.092 g, 0.17 mmol) were stirred in dichloromethane (20 mL). The initially bright-red solution became dark, and a dark-red precipitate appeared as the reaction proceeded. After 1 h, this was collected, washed with dichloromethane, and dried under vacuum: 0.038 g, 24%; UV λ_{max} (CH_2Cl_2) 376 Soret, 500, 574 nm; IR (KBr) 1565 vs (OEP•) cm^{-1}. Anal. Calcd for $C_{36}H_{44}N_4Cl_{66}NiSb$: C, 46.70; H, 4.79; N, 6.05. Found: C, 47.05; H, 4.86; N, 6.06. [Ni(TMP•)][SbCl$_6$] was characterized spectroscopically: λ_{max} (CH_2Cl_2) 397 Soret, 643 nm.

[Co(TPP•)][SbCl$_6$]·0.5CH$_2$Cl$_2$. Co(TPP) (0.10 g, 0.15 mmol) and tris(*p*-bromophenyl)aminium hexachloroantimonate[9] (0.073 g, 0.15 mmol) were stirred in dichloromethane (20 mL) until all the reactants were dissolved (15 min). The solution was filtered through a fine frit, and heptane (30 mL) was added. The resulting purple precipitate was immediately collected and washed with heptane: 0.11 g, 70%; UV λ_{max} (CH_2Cl_2) 398 Soret, 542, 610, 645 nm; IR (KBr) 1290 (TPP•) cm^{-1}. Anal. Calcd for $C_{44.5}H_{29}N_4Cl_7Sb$: C, 50.97; H, 2.78; N, 5.34. Found: C, 51.13; H, 3.04; N, 5.28. Preparations of [Co(TPP•)][SbCl$_6$] using phenoxathiinylium hexachloroantimonate gave elemental analyses indicative of phenoxathiin inclusion perhaps as an axial ligand. The analogous *p*-tolylporphyrin species was found to have essentially identical spectroscopic properties and was used for an ^{1}H NMR determination of μ_{eff} = 2.5 μ_B at 303 K.

Table I. Summary of Crystal Data and Intensity Collection Parameters for [Cu(TPP•)]SbCl$_6$

formula	$CuN_4C_{44}H_{28}SbCl_6$
fw, amu	1010.74
crystal dimensions, mm	0.16 × 0.30 × 0.39
space group	$P\bar{1}$
temp, K	293
a, Å	13.484 (2)
b, Å	13.924 (3)
c, Å	12.886 (2)
α, deg	98.90 (2)
β, deg	111.08 (1)
γ, deg	106.97 (2)
V, Å^3	2065.7
Z	2
d_{calcd}, g/cm^3	1.625
d_{obsd}, g/cm^3	1.63
radiation	graphite-monochromated Mo Kα (0.71073 Å)
scan technique	θ–2θ
scan range	0.7° below K_{α_1} to 0.7° above K_{α_2}
scan range, deg/min	2–12
bckgrd	one-half scan time at extremes of scan
2θ limits, deg	$F_o > 3\sigma(F_o)$
unique obsd data	3934
μ, mm^{-1}	1.60 (empirical correction)
R_1	0.091
R_2	0.087
goodness of fit	2.129

Magnetic Susceptibility. Measurements were performed on finely ground samples (0.030 g) in aluminum or Kel-F buckets on an SHE Model 905 Squid susceptometer operating at 10 kG. Sample integrity was checked after measurement by UV-vis spectroscopy. Diamagnetic corrections (χ_{dia}) were calculated by using the published value for the constitutive correction for H_2TPP[10] and Pascal's constants. Specific values are given above. Ambient temperature gram susceptibilities of -10^{-6} cgs units (or of greater magnitude) were taken to indicate diamagnetism. Listings of magnetic susceptibility data for [Cu(TMP•)][SbCl$_6$]·C$_6$H$_5$F and [VO(TPP•)][SbCl$_6$] are given in the supplementary material, and the data are displayed graphically in the text. Evans method determinations of solution susceptibilities were performed in the usual manner on a Varian XL 100 spectrometer using dichloromethane-d_2 containing 1% Me_4Si. The following values of μ_{eff} for [Cu(TPP•)][SbCl$_6$] were obtained as a function of temperature (K): 2.37 (303), 2.27 (283), 2.21 (273), 2.15 (263), 2.08 (253), 1.99 (243), 1.09 (233), 1.79 (223), 1.66 (213), 1.56 (203) μ_B.

X-ray Structure Determination of [Cu(TPP•)][SbCl$_6$]. Single crystals were grown by heptane layering of a dichloromethane solution of the complex. Preliminary photographic examination of the crystals suggested a two-molecule triclinic unit cell, space group *P*1 or $P\bar{1}$. Final lattice constants and intensity data collection parameters are summarized in Table I. A Delauney reduction using the final cell parameters confirmed the triclinic description of the unit cell. All measurements utilized a Nicolet P1 diffractometer.

The initial choice of the centrosymmetric space group $P\bar{1}$ was fully confirmed by all subsequent developments during the determination of structure. The structure was solved by standard heavy-atom methods[12] and refined by full-matrix least-squares techniques. Difference Fourier calculations revealed electron density contributions appropriately located for all hydrogen atom positions. These were included as fixed idealized (d(C–H) = 0.95 Å) contributors in all subsequent least-squares calculations. Final statistics for the converged anisotropic model are presented

(5) Adler, A. D.; Longo, F. R.; Finarelli, J. D.; Goldamacher, J.; Assour, I.; Korsakoff, L. *J. Org. Chem.* **1967**, *32*, 476.
(6) Barnett, G. M.; Hudson, M. F.; Smith, K. M. *Tetrahedron Lett.* **1973**, *17*, 1028.
(7) Groves, J. T. *J. Am. Chem. Soc.* **1983**, *105*, 6243.
(8) Perrin, D. D.; Armarego, W. L. F.; Perrin, D. R. *Purification of Laboratory Chemicals*; Pergamon: New York, 1980.
(9) Bell, F. A.; Ledwith, A.; Sherrington, D. C. *J. Chem. Soc. B* **1969**, 2719.
(10) Eaton, S. S.; Eaton, G. R. *Inorg. Chem.* **1980**, *19*, 1095.
(11) Evans, D. F. *J. Chem. Soc.* **1959**, 2003.
(12) Programs used in this study included local modifications of Jacobson's ALLS, Zalkin's FORDAP, Busing and Levy's ORFFE and ORFLS, and Johnson's ORTEP2. Atomic form factors were from: Cromer, D. T.; Mann, J. B. *Acta Crystallogr., Sect. A: Cryst. Phys., Diffr., Theor. Gen. Crystallogr.* **1968**, *A24*, 321. Real and imagnary corrections for anomalous dispersion in the form factor of the antimony, copper, and chlorine atoms were from: Cromer, D. T.; Liberman, D. J. *J. Chem. Phys.* **1970**, *53*, 1891. Scattering factors for hydrogen were from: Stewart, R. F.; Davidson, E. R.; Simpson, W. T. *Ibid.* **1965**, *42*, 3175.

Table II. Fractional Atomic Coordinates in the Unit Cell of [CuTPP][$SbCl_6$][a]

atom	10^4x	10^4y	10^4z
Cu	3348 (1)	651 (1)	-1231 (1)
N_1	3563 (7)	2010 (6)	-1611 (7)
N_2	4129 (7)	283 (6)	-2185 (7)
N_3	3173 (7)	-687 (6)	-817 (7)
N_4	2639 (7)	1073 (6)	-219 (7)
C_{a1}	3379 (9)	2849 (8)	-1083 (9)
C_{a2}	4332 (9)	2445 (8)	-2042 (9)
C_{a3}	4415 (9)	804 (8)	-2933 (9)
C_{a4}	4099 (9)	-724 (8)	-2597 (9)
C_{a5}	3617 (9)	-1410 (7)	-1117 (9)
C_{a6}	2908 (9)	-923 (8)	82 (9)
C_{a7}	2144 (9)	476 (8)	333 (9)
C_{a8}	2204 (9)	1880 (8)	-222 (9)
C_{b1}	4075 (9)	3791 (8)	-1156 (10)
C_{b2}	4673 (9)	3577 (8)	-1712 (10)
C_{b3}	4506 (10)	134 (9)	-3813 (8)
C_{b4}	4321 (10)	-811 (8)	-3589 (10)
C_{b5}	3632 (10)	-2080 (8)	-386 (10)
C_{b6}	3219 (10)	-1778 (8)	346 (10)
C_{b7}	1390 (10)	842 (9)	636 (10)
C_{b8}	1422 (10)	1683 (9)	265 (10)
C_{m1}	4644 (9)	1887 (8)	-2766 (9)
C_{m2}	3936 (9)	-1502 (8)	-2036 (9)
C_{m3}	2373 (8)	-438 (8)	591 (9)
C_{m4}	2614 (9)	2750 (8)	-580 (9)
C_1	5266 (9)	2437 (7)	-3377 (9)
C_2	6288 (10)	2418 (8)	-3318 (9)
C_3	6902 (10)	3019 (9)	-3807 (10)
C_4	6431 (13)	3644 (10)	-4408 (11)
C_5	5390 (13)	3652 (10)	-4496 (12)
C_6	4794 (11)	3062 (9)	-4005 (11)
C_7	4182 (10)	-2456 (8)	-2377 (9)
C_8	3393 (11)	-3444 (9)	-2630 (10)
C_9	3722 (13)	-4317 (9)	-2865 (11)
C_{10}	4764 (14)	-4150 (11)	-2838 (12)
C_{11}	5535 (12)	-3176 (12)	-2638 (12)
C_{12}	5239 (11)	-2316 (9)	-2366 (10)
C_{13}	1959 (9)	-874 (9)	1394 (10)
C_{14}	1263 (10)	-1913 (10)	1057 (11)
C_{15}	855 (11)	-2309 (12)	1832 (16)
C_{16}	1133 (14)	-1666 (15)	2890 (16)
C_{17}	1793 (14)	-696 (14)	3224 (14)
C_{18}	2233 (11)	-248 (10)	2472 (12)
C_{19}	2222 (9)	3637 (8)	-410 (10)
C_{20}	2265 (11)	4099 (10)	648 (12)
C_{21}	1925 (13)	4918 (10)	798 (14)
C_{22}	1529 (13)	5303 (10)	-190 (17)
C_{23}	1478 (13)	4857 (11)	-1256 (15)
C_{24}	1833 (11)	4038 (10)	-1365 (12)
Sb	442 (1)	2508 (1)	3936 (1)
Cl_1	-540 (4)	2930 (4)	2252 (4)
Cl_2	-13 (6)	867 (4)	2765 (5)
Cl_3	1457 (4)	2133 (5)	5625 (4)
Cl_4	887 (7)	4218 (6)	5021 (7)
Cl_5	-1236 (4)	1897 (6)	4148 (5)
Cl_6	2142 (4)	3178 (6)	3720 (5)

[a] The numbers in parentheses are the estimated standard deviations in the least significant figure.

in Table I. Final values of the atomic coordinates are reported in Table II. Final values of anisotropic thermal parameters and fixed hydrogen atom positions are reported in Tables IS and IIS of the supplementary material. Tables IIIS and IVS contain nonessential bond lengths and bond angles, respectively.

Although bulk samples gave elemental analyses indicating up to 0.5 CH_2Cl_2 solvate, no solvent molecules were found in the lattice of the single crystal used in this study. We have observed this phenomenon previously[2] and assume that random solvate inclusion is more prevalent in less well-formed crystals. The [Cu(TPP$^{\bullet}$)][$SbCl_6$] lattice was carefully examined[13] for hole(s) that could accommodate CH_2Cl_2 molecules. No cavity large enough was found, although the cavities in the crystalline lattice were somewhat larger than normally found in porphyrin lattices.

(13) Use was made of the program CAVITY, briefly described by Basso: Basso, R.; Della Giusta, A. *J. Appl. Crystallogr.* **1977**, *10*, 496.

Results and Discussion

General. Much of the early work on metalloporphyrin π-cation radicals relied upon electrochemical synthesis together with characterization by solution spectroscopic methods.[14,15] There are some shortcomings to this approach as perhaps best illustrated by the decade-long uncertainty about the true nature of [FeCl(TPP)]$^+$, now conclusively shown to be an iron(III) porphyrin π-cation radical rather than an iron(IV) porphyrin.[2] The problems become particularly evident when probing magnetic properties because reliable measurements of magnetic susceptibility in solution require excellent purity, good solubility, and reasonable compound lifetime. Most metalloporphyrin π-cation radicals, however, are rather unstable in solution. We have therefore concentrated our efforts on synthetic methods which lead to isolable crystalline solids of analytical purity. The most significant advance to this end was recognizing the utility of certain stable organic radical salts, ($R^{\bullet+}$)Y, as convenient oxidants of measurable one-electron potential:

$$M(TPP) + (R^{\bullet+})Y \rightarrow [M(TPP^{\bullet})]Y + R$$

R is usually phenoxathiin but sometimes thianthrene or tris(*p*-bromophenyl)amine in the present work, and Y is $SbCl_6^-$ or ClO_4^-. The $R/R^{\bullet+}$ redox potentals in dichloromethane are all ca. 1.20 V relative to SCE which conveniently puts them just above most $M(TPP)/M(TPP^{\bullet})^+$ potentials.[14] These reagents allow one to do the synthetic equivalent of controlled potential electrolysis without the complication of an electrolyte. We have also found that the choice of solvent is important. For reasons that remain obscure some metalloporphyrin radicals are very much less stable than others. Their rapid isolation by using poorly solvating solvents such as carbon tetrachloride and fluorobenzene has proved important for obtaining materials of analytical purity.

In order to establish that the site of oxidation is the porphyrin ring rather than the metal we have relied mainly on UV–vis and IR criteria. UV–vis criteria tend to be reliable when the metal is diamagnetic and/or when its oxidation potential is far removed from that of the porphyrin (e.g., Cu and Zn). A dramatic intensity lowering and blue-shifting of the Soret band relative to the unoxidized precursor is typical as is a broadening of the lower energy α,β region. Sometimes there is the appearance of a relatively strong absorption above 600 nm. For the more redox-active metals, such as Cr, Mn, Fe, Co, and Ni, these features may be much less pronounced, and corroborating evidence is required. We have proposed that IR spectroscopy provides a new and convenient diagnostic band for porphyrin vs. metal oxidation.[16] A strong absorption near 1290 cm^{-1} is seen in $TPP^{\bullet+}$ complexes and near 1560 cm^{-1} in $OEP^{\bullet+}$ complexes. Despite the fact that these bands were identified as porphyrin modes by their shifts to lower frequencies with pyrrole ring deuteriation,[16] it has been suggested[17] that they might be ascribed to absorptions of chlorinated hydrocarbon solvate molecules. Although this may be the case for [MnCl(TPP)][$SbCl_6$] where the 1285-cm^{-1} band is of medium intensity, all of the present metalloporphyrin radical complexes show the diagnostic band with very strong intensity, including some which lack chlorinated hydrocarbon solvates in their solid-state elemental composition. Moreover, when [FeCl(TPP$^{\bullet}$)][$SbCl_6$], which contains no more than one-fourth CH_2Cl_2 of solvation,[2] is synthesized and crystallized from 99% deuterio CH_2Cl_2-d_2 the diagnostic band is undiminished relative to the same material isolated under identical conditions in protio CH_2Cl_2. This is illustrated in Figure 1. This leads us to reaffirm the utility of IR for identifying porphyrin ring oxidation, and the present work extends the use of the 1290-cm^{-1} band of $TPP^{\bullet}$ to its mesityl analogue $TMP^{\bullet}$.

Copper. There can be little doubt now that the oxidation of copper(II) porphyrins is ring centered rather than metal cen-

(14) Wolberg, A.; Manassen, J. *J. Am. Chem. Soc.* **1970**, *92*, 2982.
(15) Fuhrhop, J.-H. *Struct. Bonding (Berlin)* **1974**, *18*, 1.
(16) Shimomura, E. T.; Phillippi, M. A.; Goff, H. M.; Scholz, W. F.; Reed, C. A. *J. Am. Chem. Soc.* **1981**, *103*, 6778.
(17) Spreer, L. O.; Maliyackel, A. C.; Holbrook, S.; Otvos, J. W.; Calvin, M. *J. Am. Chem. Soc.* **1986**, *108*, 1949.

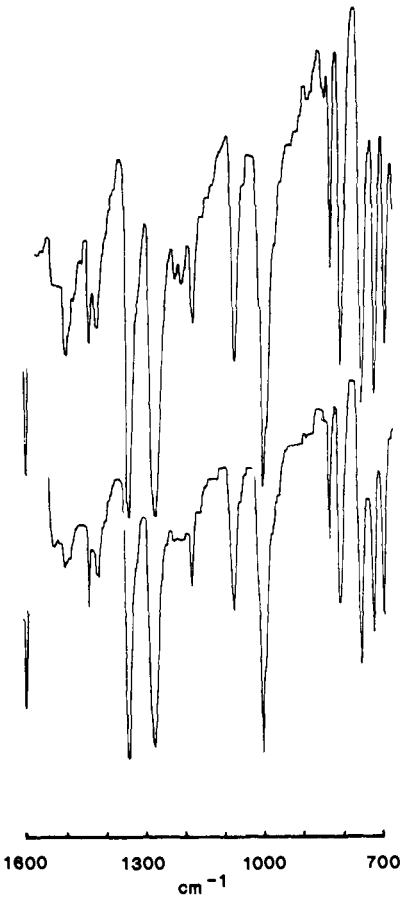

Figure 1. Comparison of IR spectra (KBr) for $[FeCl(TPP^{\bullet})][SbCl_6]$ prepared from dichloromethane (upper) and 99% deuterio dichloromethane (lower). Differences are considered to be insignificant. Calibration spikes are the 1601-cm^{-1} band of polystyrene.

tered.[14,15] The π-cation radical formulation is supported by IR, UV–vis, and X-ray criteria in the present work as well as by NMR,[18] RR,[19] and MCD[20] in other recent work.

On the other hand, the reported magnetic data on copper(II) porphyrin cation radical species present a confusing picture. In solution, $[Cu(TPP^{\bullet})]^+$ has been reported to have μ_{eff} values of 2.88,[14] 0,[21] 2.4,[4] 2.9,[22] and 2.4[18] μ_B. Part of the explanation for this range of values probably lies in experimental difficulties with the Evans method and the sensitivity of the materials to errant nucleophiles. But there is also evidence for aggregation. In CD_2Cl_2 solution we find by the Evans method that μ_{eff} decreases from 2.37 μ_B at 303 K to 1.56 μ_B at 203 K. A reasonable explanation for such a large decrease is an intermolecular antiferromagnetic coupling caused by association into dimeric units. A definitive Beer's law investigation was not practical, but there is more than ample literature precedent for dimerization of porphyrins and porphyrin π-cation radicals.[23] Moreover, the X-ray crystal structure of $[Cu(TPP^{\bullet})][SbCl_6]$ reveals dimers that are diamagnetic. Aggregation effects might also help to explain the difficulty of locating the β-pyrrole resonance in the ^1H NMR spectrum.[18] Significantly higher temperatures were not accessible in our Evans method NMR experiments, so it is not possible to know what the maximum μ_{eff} value might be in dichloromethane. One of the reported values[14] of 2.9 μ_B was obtained in the presence of an electrolyte in benzonitrile solution where the existence of a nonaggregated species is more likely than in dichloromethane. In view of the 2.9 value obtained with the mesitylporphyrin analogue (in the more reliable solid-state measurements, see below) we suspect that μ_{eff} for a truly monomeric $[Cu(TPP^{\bullet})]^+$ cation may be 2.9 μ_B.

In analogous investigations with octaethylporphyrin derivatives, a variety of differing observations have been reported. In frozen solution, there is good evidence from EPR spectroscopy[24] that monomeric $[Cu(OEP^{\bullet})]^+$ has a triplet ground state. A magnetic moment of 2.9 μ_B might therefore be expected. The most recently measured value is 2.3 μ_B.[18] This moment has been rationalized on the basis of nonaggregated molecules with noninteracting spins (μ_{theory} = 2.45 μ_B).[25] However, we suspect that this ambient temperature moment is affected by solution aggregation phenomena since aggregation is proven at low temperature.[18,23] Moreover, the room temperature solid-state moment of $[Cu(OEP^{\bullet})][SbC_6]$, which is known to be dimeric from EPR measurements, is 1.95 μ_B.[26]

The above conclusions suggested that a clearer picture of the spin coupling between copper(II) and its ligand radical would be possible if complications from aggregation were removed. To this end we have prepared the analogous tetramesitylporphyrin derivative $[Cu(TMP^{\bullet})]^+$, anticipating that the peripheral steric bulk of the *o*-methyl groups above and below the porphyrin plane would effectively isolate each metalloporphyrin molecule from even weak intermolecular interactions. The evidence from solid-state magnetic susceptibility measurements on $[Cu(TMP^{\bullet})][SbCl_6]\cdot C_6H_5F$ is that a magnetically dilute system has indeed been achieved. The μ_{eff} value is 2.9 ± 0.16 μ_B throughout the entire temperature range 6–300 K, and the Curie plot is essentially linear (Figure 2). This is what is expected for an S = 1 triplet ground state without significant population of the singlet state. A conservative estimate of the triplet–singlet energy gap $+2J$ is 400 cm^{-1}, but it may be >1000 cm^{-1}. The difficulty in determining this value accurately arises from the sensitivity of the high-temperature susceptibility data to one's estimate of the diamagnetic correction and TIP.

With definitive evidence from magnetic susceptibility for the S = 1 (triplet) state, a new picture of *paramagnetic* copper(II) porphyrin cation radicals is emerging. There is no longer any need to retain the possibility of noninteracting spins since all published moments lower than 2.9 μ_B can be understood in terms of aggregation effects. One caveat worth noting, however, is that the presence of a low-lying intramolecular S = 0 (singlet) state would be difficult to distinguish from aggregation effects. Nevertheless, triplet ground states prevail in site-isolated $[Cu(porph^{\bullet})]^+$ cations, and the triplet–singlet splitting energy of >400 cm^{-1} found for the mesitylporphyrin derivative reveals a substantial stabilization of the spin-parallel state. Further evidence for the ferromagnetically coupled state comes from ^1H NMR shifts of the phenyl protons in $M(TPP^{\bullet+})$ species. Like the ferromagnetically coupled $Fe(OClO_3)_2(TPP^{\bullet})$,[4] the ortho and para protons of $[Cu(TPP^{\bullet})]^+$ are upfield shifted, and the meta protons are downfield shifted relative to the unoxidized precursor.[17] The opposite pattern is observed for the antiferromagnetically coupled $[FeCl(TPP^{\bullet})]^+$. It appears that a diagnostic pattern is emerging, at least for overall integral spin states. There is a good basis for expecting this generality because hyperfine coupling constants are known to switch sign when the overall spin state changes from higher to lower multiplicity.[27]

The rationale for the triplet ground state lies in the orthogonality of the magnetic orbitals. Making the reasonable assumption that site-isolated $[Cu(porph^{\bullet})]^+$ units will have local D_{4h} symmetry, we see that the metal $d_{x^2-y^2}$ orbital (b_{1g}) is orthogonal to the

(18) Godziela, G. M.; Goff, H. M. *J. Am. Chem. Soc.* **1986**, *108*, 2237.
(19) Yamaguchi, H.; Nakano, M.; Itoh, K. *Chem. Lett.* **1982**, 1397.
(20) Browett, W.; Stillman, M. J. *Inorg. Chim. Acta* **1977**, *49*, 69.
(21) Dolphin, D.; Muljiani, Z.; Rousseau, K.; Borg, D. C.; Fajer, J.; Felton, R. H. *Ann. N. Y. Acad. Sci.* **1973**, *206*, 177.
(22) Carnieri, N.; Harriman, A. *Inorg. Chim. Acta* **1982**, *62*, 103.
(23) Mengersen, C.; Subramanian, J.; Fuhrhop, J.-H. *Mol. Phys.* **1976**, *32*, 893.
(24) Konishi, S.; Hoshimo, M.; Imamura, M. *J. Am. Chem. Soc.* **1982**, *104*, 2057. The unusual monomeric nature of this radical results for γ radiolysis of a frozen tetrachloroethane matrix.
(25) μ is calculated as the square root of the sum of the squares of the moments of the independent spins.
(26) Mondal, J. U.; Scheidt, W. R., unpublished observations.
(27) Gateschi, D.; Bencini, A. *Magneto-Structural Correlations in Exchange Coupled Systems*; Willett, R. D., Gatteschi, D., Kahn, O., Eds.; Reidel: Dordrect, Netherlands, 1985, 241.

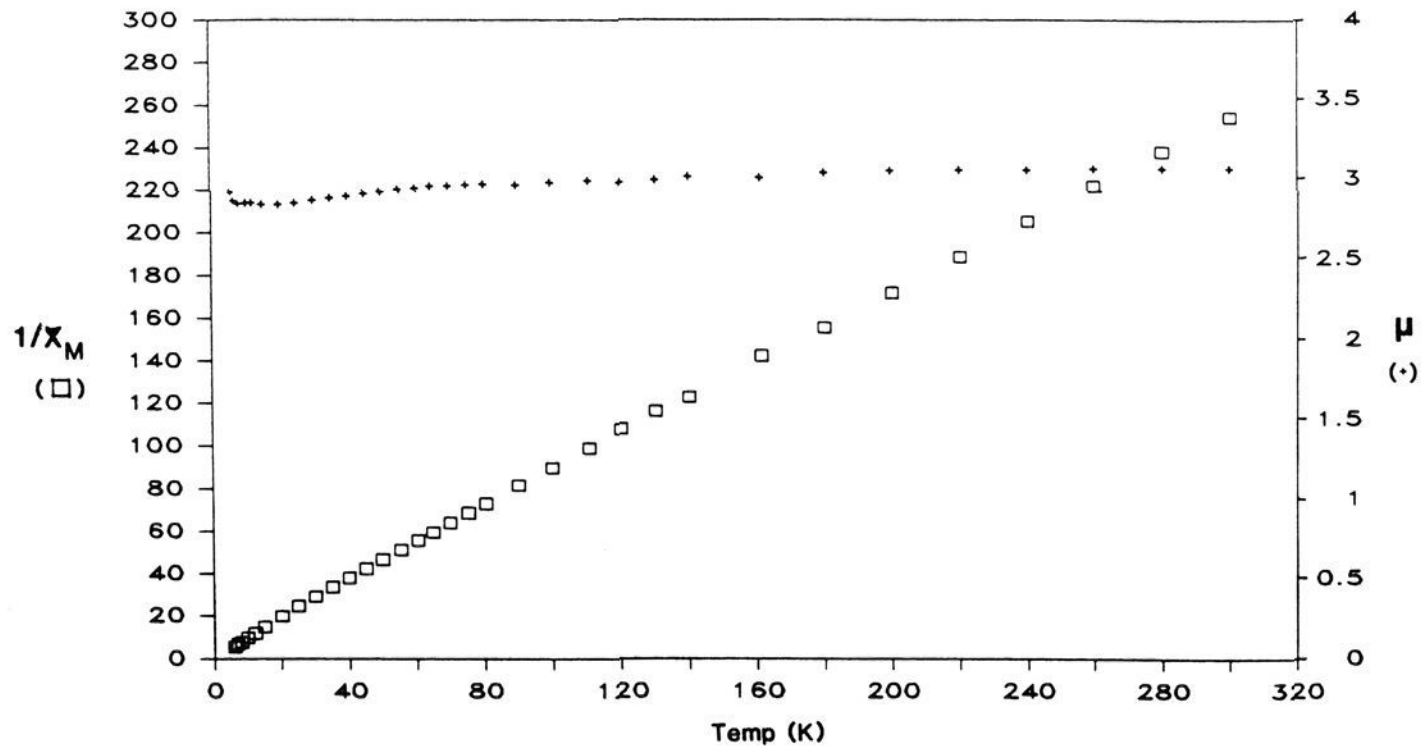

Figure 2. Curie plot (□) and μ_{eff} vs. temperature (+) for $[Cu(TMP^{\bullet})][SbCl_6]\cdot C_6H_5F$.

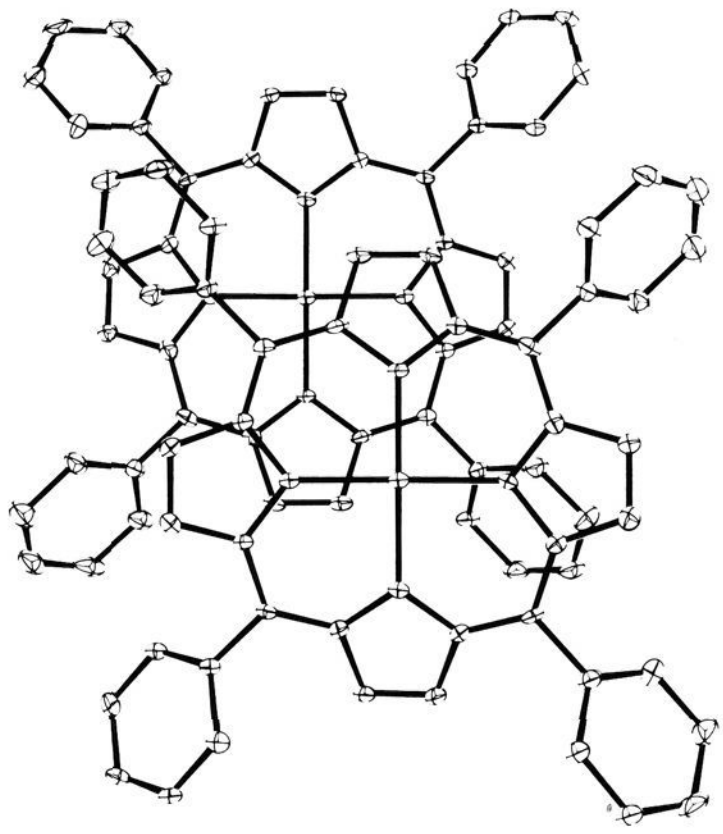

Figure 3. View of the solid-state interaction between two $[Cu(TPP^{\bullet})]^+$ ions. The lower (left-hand) ion is drawn such that its mean plane is parallel to the plane of the paper; the centrosymmetric relationship between the two ions ensures that the upper mean plane core is also parallel to the paper plane.

porphyrin HOMO (a_{1u} or a_{2u}). In fact, $[Cu(TPP^{\bullet})]^+$ has been analyzed by UV–vis[21] and NMR[18] spectroscopies to be of the a_{2u} type, although an a_{1u} assignment has been suggested[18] for $[Cu(OEP^{\bullet})]^+$. This does not alter the symmetry argument, but we might expect the triplet–singlet energy gap to decrease in an a_{1u} type species since it localizes less unpaired electron spin density at the porphinato nitrogen atoms than does an a_{2u} type radical.[28] In the language of magnetic interactions the metal and ligand spins are ferromagnetically coupled via an exchange interaction.

We turn now to the structure of $[Cu(TPP^{\bullet})][SbCl_6]$, which is a diamagnetic substance in the solid state. A most important feature of the solid-state structure is the appearance of tightly associated pairs of cations. The formation of this dimer has important consequences for the detailed stereochemistry of the $[Cu(TPP^{\bullet})]^+$ cation (see below). The face-to-face structure of the dimer (shown in Figure 3) lacks any recognizable specific HOMO–LUMO interaction or any intermolecular metal–nitrogen interactions. The driving force for dimerization is probably best

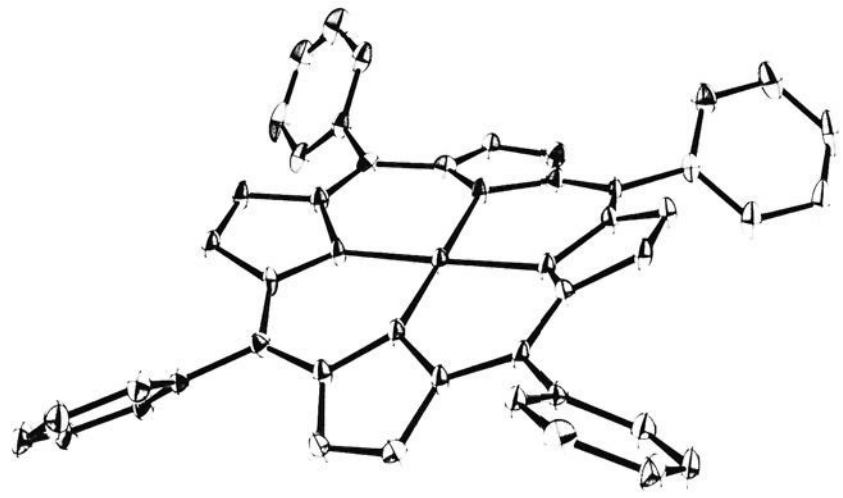

Figure 4. ORTEP2 diagram of an isolated $[Cu(TPP^{\bullet})]^+$ ion showing the extreme nonplanar nature of the species. Ellipsoids are contoured at the 50% probability level.

viewed as $\pi-\pi$ bond formation between two half-occupied porphyrin HOMOs. The importance of this paired interaction on the magnetic coupling of the ion will be discussed subsequently.

The overall conformation of the $[Cu(TPP^{\bullet})]^+$ ion is quite distinctive compared with many other porphinato derivatives. The conformation is distinctive on three counts: (i) the large magnitude of the displacement of the core atoms from the mean plane, (ii) the pattern of displacements of the pyrrole rings, and (iii) the unusually small values for the phenyl group dihedral angles. As discussed below, we note that these conformational features are required to allow even the moderately close (3.84 Å) interplanar spacing between the two cores observed and illustrated in Figure 3. The extreme nonplanarity of the ion is illustrated in Figure 4, and a quantitative description of the ruffling of the core is shown in Figure 5. In Figure 5, each atomic position has been replaced by the value of the perpendicular displacement (in units of 0.01 Å) of each atom from the mean plane of the core. The quasi-D_{2d}-ruffled core of this species has the pyrrole rings displaced, alternately, above and below the mean plane of the core. This conformation differs from the more usual D_{2d}-ruffled cores by a 45° rotation of the point group symmetry operators around the major twofold axis (perpendicular to the mean plane). We believe that this core conformation (the unusual saddle-shaped ruffling) results from the necessity of making the bulky peripheral phenyl groups more nearly coplanar with the porphinato core. This coplanarity of the phenyl groups is needed to allow the close porphyrin core contacts found in the dimer. As detailed for a number of other porphyrin derivatives,[29] the most reasonable stereochemical pathway for achieving phenyl ring near coplanarity

(28) Gouterman, M. *J. Mol. Spectrosc.* **1961**, *6*, 138.

(29) Scheidt, W. R.; Lee, Y. J. *Struct. Bonding* (*Berlin*), in press.

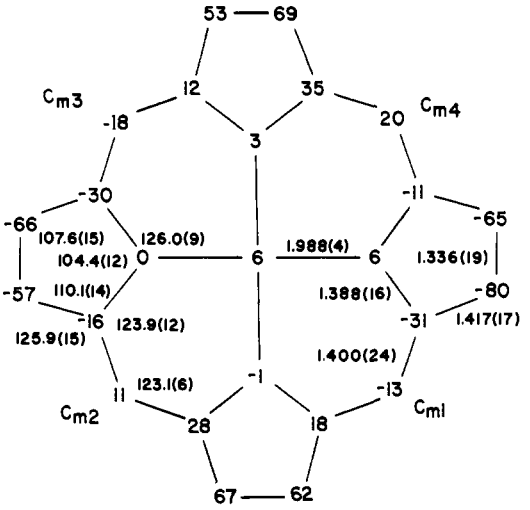

Figure 5. Formal diagram of the porphinato core in [Cu(TPP•)][$SbCl_6$] displaying the perpendicular displacements (in units of 0.01 Å) of each atom from the mean plane of the core. Also displayed are the averaged values of the chemically distinct bond distances and angles of the core. The numbers in parentheses are estimated standard deviations, calculated on the assumption that the averaged values are all drawn from the same population.

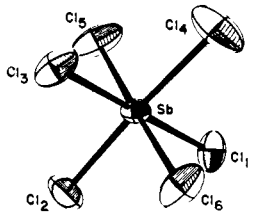

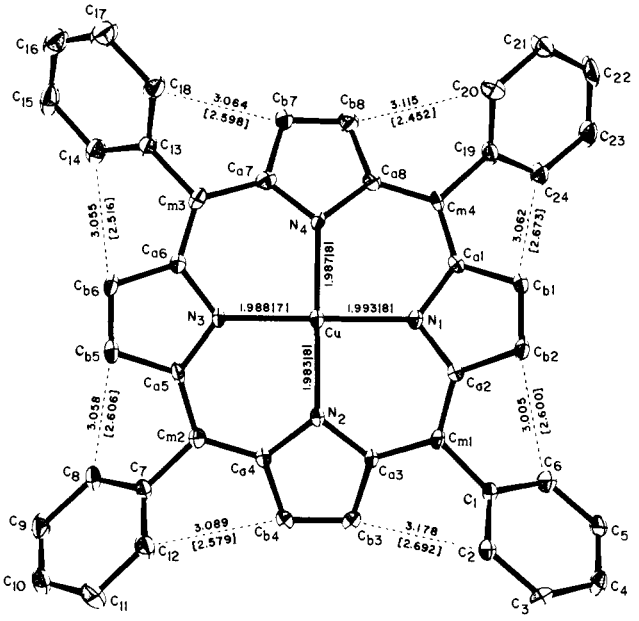

Figure 6. Diagram illustrating the nonbonded distances between ortho phenyl carbon atoms and the C_b atoms of the porphyrin. The analogous H···H contacts are given in square brackets. Also shown is the labeling scheme for all unique atoms in the structure.

is through a saddle-shaped deformation of the core. The importance of the saddle-shape conformation in allowing near coplanarity of the phenyl groups is shown in Figure 6, which displays the C···C contacts between the ortho phenyl carbon atoms and the C_b core carbon atoms.[30] Also displayed in the figure (inside the square brackets) are the analogous H···H distances (based on the idealized hydrogen atom positions). The figure makes clear the importance of the vertical tilt of the pyrrole rings in maximizing the ortho phenyl atom contacts with the porphinato core. A careful examination of Figure 6 reveals that the rotation sense of any adjacent pair of phenyl rings is such that the tight phenyl carbon interactions are both on the same side of the relevant pyrrole ring. It should be emphasized that the constraints of the porphyrin macrocycle probably require the propagation of the ruffling around the entire core perimeter once it starts between a pair of pyrrole rings. The values of the dihedral angles between the mean core and the phenyl rings are 41.7°, 42.6°, 43.0°, and 38.6°. The usually observed value for this angle is > 60°.

Table III. Selected Bond Lengths in [CuTPP][$SbCl_6$][a]

type	length, Å	type	length, Å
$Cu-N_1$	1.993 (8)	$C_{a3}-C_{b3}$	1.418 (13)
$Cu-N_2$	1.983 (8)	$C_{a3}-C_{m1}$	1.412 (13)
$Cu-N_3$	1.988 (7)	$C_{a4}-C_{b4}$	1.410 (13)
$Cu-N_4$	1.987 (8)	$C_{a4}-C_{m2}$	1.400 (13)
N_1-C_{a1}	1.392 (11)	$C_{a5}-C_{b5}$	1.424 (13)
N_1-C_{a2}	1.379 (11)	$C_{a5}-C_{m2}$	1.398 (13)
N_2-C_{a3}	1.388 (11)	$C_{a6}-C_{b6}$	1.423 (13)
N_2-C_{a4}	1.404 (12)	$C_{a6}-C_{m3}$	1.376 (13)
N_3-C_{a5}	1.386 (11)	$C_{a7}-C_{b7}$	1.405 (13)
N_3-C_{a6}	1.388 (12)	$C_{a7}-C_{m3}$	1.453 (13)
N_4-C_{a7}	1.358 (12)	$C_{a8}-C_{b8}$	1.394 (13)
N_4-C_{a8}	1.411 (12)	$C_{a8}-C_{m4}$	1.398 (13)
$C_{a1}-C_{b1}$	1.412 (13)	$C_{b1}-C_{b2}$	1.320 (13)
$C_{a1}-C_{m4}$	1.387 (13)	$C_{b3}-C_{b4}$	1.362 (13)
$C_{a2}-C_{b2}$	1.450 (13)	$C_{b5}-C_{b6}$	1.330 (13)
$C_{a2}-C_{m1}$	1.378 (12)	$C_{b7}-C_{b8}$	1.326 (13)

[a] The numbers in parentheses are the estimated standard deviations in the least significant figure.

To varying degrees the above conformational aspects and dimer formation are a feature of all but one of the four- and five-coordinate metalloporphyrin π-cation radicals that have been crystallographically characterized: [FeCl(TTP•)][$SbCl_6$][2,31] (3.68, 4.70), [Zn(TPP•)($OClO_3$)][32] (3.70, 6.54), and [Mg(TPP•)($OClO_3$)][33] (3.77, 6.67). The numbers in parentheses following each compound are, respectively, the mean plane separation and the center–center distance in each dimer (in Å). The corresponding values for [Cu(TPP•)]$^+$ are 3.84 and 5.40 Å. We note that the unusual saddle-shaped core conformation of the π-cation radicals is thus an adaptation to allow dimer formation. We expect that this saddle-shaped core will be found for *meso*-arylporphyrins and not porphyrin derivatives with alkyl substituents. Further, differences[29] in the geometry of dimers formed by alkyl-substituted vs. *meso*-aryl-substituted porphyrins may lead to differences in the nature of the intermolecular π–π coupling. This question remains under investigation in these laboratories.

The stereochemical features of the [Cu(TPP•)]$^+$ ion are otherwise typical of those expected for Cu(porph) species. Figure 5 summarizes averaged values for chemically equivalent bond distances and angles, and individual values are tabulated in Tables III and IV. The average Cu–N bond distance of 1.988 (4) Å is quite comparable to values reported previously: 1.981 (7) Å for ruffled Cu(TPP),[34] 2.000 (5) Å for planar Cu(TPrP),[35] 1.987 (8) Å for a face-to-face derivative,[36] and 1.997 (4) Å in a biphenylene-pillared biporphyrin.[37] The Cu–N bond distance is thus quite consistent with a ring-oxidized derivative and not a

(30) It can be noted that the phenyl carbon to C_a distances are generally slightly shorter than the C_b values given in Figure 6.

(31) Lang, G.; Boss, B.; Erler, B. S.; Reed, C. A. *J. Chem. Phys.* **1986**, *84*, 2998.
(32) Spaulding, L. D.; Erler, P. G.; Bertrand, J. A.; Felton, R. H. *J. Am. Chem. Soc.* **1974**, *96*, 982.
(33) Barkigia, K. M.; Spaulding, L. D.; Fajer, J. *Inorg. Chem.* **1983**, *22*, 349.
(34) Fleischer, E. B.; Miller, C. K.; Webb, L. E. *J. Am. Chem. Soc.* **1964**, *86*, 2342.
(35) Moutakali, I.; Tulinsky, A. *J. Am. Chem. Soc.* **1973**, *95*, 6811.
(36) Collman, J. P.; Chong, A. O.; Jameson, G. B.; Oakley, R. T.; Rose, E.; Schmittou, E. R.; Ibers, J. A. *J. Am. Chem. Soc.* **1981**, *103*, 516.
(37) Fillers, J. P.; Ravichandran, K. G.; Abdalmuhdi, I.; Tulinsky, A.; Chang, C. K. *J. Am. Chem. Soc.* **1986**, *108*, 417.

Table IV. Selected Bond Angles in [CuTPP][$SbCl_6$][a]

type	angle, deg	type	angle, deg
N_1CuN_2	89.5 (3)	$C_{m3}C_{a7}C_{b7}$	123.6 (9)
N_1CuN_3	178.5 (4)	$N_4C_{a8}C_{m4}$	122.2 (9)
N_1CuN_4	89.5 (3)	$N_4C_{a8}C_{b8}$	108.6 (9)
N_2CuN_3	90.4 (3)	$C_{74}C_{a8}C_{b8}$	129.0 (10)
N_2CuN_4	177.2 (4)	$C_{a1}C_{b1}C_{b2}$	109.3 (9)
N_3CuN_4	90.4 (3)	$C_{a2}C_{b2}C_{b1}$	106.6 (9)
$C_{a1}N_1C_{a2}$	105.2 (8)	$C_{a3}C_{b3}C_{b4}$	106.4 (9)
$C_{a3}N_2C_{a4}$	103.2 (8)	$C_{a4}C_{b4}C_{b3}$	107.6 (9)
$C_{a5}N_3C_{a6}$	105.6 (8)	$C_{a5}C_{b5}C_{b6}$	108.1 (9)
$C_{a7}N_4C_{a8}$	103.5 (8)	$C_{a6}C_{b6}C_{b5}$	107.8 (9)
$N_1C_{a1}C_{m4}$	124.2 (8)	$C_{a7}C_{b7}C_{b8}$	105.4 (9)
$N_1C_{a1}C_{b1}$	109.3 (9)	$C_{a8}C_{b8}C_{b7}$	109.9 (10)
$C_{m4}C_{a1}C_{b1}$	126.5 (9)	$C_{a2}C_{m1}C_{a3}$	122.5 (9)
$N_1C_{a2}C_{m1}$	125.2 (9)	$C_{a2}C_{m1}C_1$	119.5 (9)
$N_1C_{a2}C_{b2}$	109.4 (8)	$C_{a3}C_{m1}C_1$	118.0 (9)
$C_{m1}C_{a2}C_{b2}$	125.1 (9)	$C_{a4}C_{m2}C_{a5}$	123.2 (9)
$N_2C_{a3}C_{m1}$	122.3 (9)	$C_{a4}C_{m2}C_7$	119.2 (9)
$N_2C_{a3}C_{b3}$	111.8 (8)	$C_{a5}C_{m2}C_7$	117.6 (9)
$C_{m1}C_{a3}C_{b3}$	125.8 (9)	$C_{a6}C_{m3}C_{a7}$	122.9 (9)
$N_2C_{a4}C_{m2}$	123.3 (9)	$C_{a6}C_{m3}C_{13}$	119.9 (10)
$N_2C_{a4}C_{b4}$	111.0 (8)	$C_{a7}C_{m3}C_{13}$	117.2 (10)
$C_{m2}C_{a4}C_{b4}$	125.6 (9)	$C_{a1}C_{m4}C_{a8}$	123.9 (9)
$N_3C_{a5}C_{m2}$	125.2 (9)	$C_{a1}C_{m4}C_{19}$	117.3 (9)
$N_3C_{a5}C_{b5}$	109.1 (9)	$C_{a8}C_{m4}C_{19}$	118.8 (9)
$C_{m2}C_{a5}C_{b5}$	125.6 (9)	CuN_1C_{a1}	125.7 (6)
$N_3C_{a6}C_{m3}$	124.9 (9)	CuN_1C_{a2}	124.2 (6)
$N_3C_{a6}C_{b6}$	109.3 (9)	CuN_2C_{a3}	126.9 (6)
$C_{m3}C_{a6}C_{b6}$	125.7 (9)	CuN_2C_{a4}	125.8 (6)
$N_4C_{a7}C_{m3}$	123.9 (9)	CuN_3C_{a5}	125.7 (6)
$N_4C_{a7}C_{b7}$	112.5 (9)	CuN_3C_{a6}	126.1 (6)
		CuN_4C_{a7}	126.9 (7)
		CuN_4C_{a8}	126.7 (8)

[a] The numbers in parentheses are the estimated standard deviations in the least significant figure.

metal-based oxidation. A d^8 Cu(III) complex would have a greatly shortened Cu–N distance due to depopulation of the antibonding $d_{x^2-y^2}$ orbital and increased metal/donor atom charge attraction. Within the precision of the experimental determination, no bond parameters of the π-cation radical differ from those appropriate for a normal porphyrin derivative.

The consequences of the interionic dimeric interaction on magnetic coupling in [Cu(TPP•)][$SbCl_6$] are complex but can probably be safely partitioned into three components: intermolecular π–π, intermolecular d–d, and intramolecular d–π. We have argued[4] that many precedents suggest that π–π coupling can be very strong. Indeed, [Ni(OEP•)][$SbCl_6$] (see later) is diamagnetic from presumed π–π coupling. It is helpful to view such antiferromagnetic coupling as nothing more than a case of weak π–π bond formation. A bond energy of only 1000 cm^{-1} (3 kcal) is enough to spin pair two interacting radicals. In the $[Cu(TPP•)]_2^{2+}$ dimer this would leave two more or less orthogonal spins in the metal $d_{x^2-y^2}$ orbitals which, because of their parallel planar orientation and their separation (Cu···Cu = 5.43 Å), are not expected to show significant coupling. So the complete diamagnetism of the dimer requires a second efficient mechanism for antiferromagnetic coupling. As with [FeCl(TPP•)][$SbCl_6$],[2,4,31] we propose that intramolecular metal–ligand spin coupling occurs as a result of the lowering of the local symmetry from D_{4h} to C_s. This destroys the orthogonality of the magnetic orbitals. Under C_s symmetry the $d_{x^2-y^2}$ and the a_{2u} orbitals both reduce to a′, and overlap becomes symmetry allowed. Even if the local symmetry was as high as C_{2v} the same would be true since both orbitals would have a_1 symmetry. The resultant spin pairing can be viewed as a metal–ligand bond with the two electrons spin paired in the bonding molecular orbital. Alternatively, it can be viewed as the dominance of an antiferromagnetic interaction (overlap) over a ferromagnetic interaction (exchange). The $S = 0$ (singlet) state is lowest in energy, and the $S = 1$ state is >1000 cm^{-1} higher in energy.

The above understanding of the two extremes of magnetic coupling allows us to anticipate the factors that would lead to intermediate cases of spin coupling. For a more minor distortion of $[Cu(porph•)]^+$ from D_{4h} symmetry one can envisage a more evenly matched competition between exchange (ferromagnetic) and overlap (antiferromagnetic) terms such that the singlet–triplet energy gap ($2J$) falls in the accessible range of kT (<1000 cm^{-1}). We can also recognize that an accidental equality of these two competing factors might lead to the appearance of noninteracting spins; i.e., the triplet and singlet states would be of equal energy. Despite the low probability of this occurring, we have in fact proposed this as the explanation for the insignificant spin coupling ($-J \simeq 2$ cm^{-1}) between iron(IV) and a porphyrin radical in horseradish peroxidase compound I.[2] The more common reason for noninteracting spins, however, will be simply that they are in molecular orbitals which are physically well separated from each other. Such a species will behave like a biradical, and the weak interactions between the unpaired electrons can be probed by ESR spectroscopy, rather than magnetic susceptibility. A recent example can be found in copper(II) complexes having nitroxyl radicals as ligands.[38]

Vanadyl. The preceding discussion introduces the possibilities for vanadylporphyrin π-cation radicals where, like copper(II), there is one unpaired electron on the metal and one on the ring. The difference lies in their relative symmetries and in the degree of interaction of the magnetic orbitals. The vanadyl d_{xy} orbital has b_2 symmetry if the molecule has local C_{4v} symmetry, and orthogonality with the porphyrin a orbital leads to the expectation of an $S = 1$ ground state. This is, in fact, the conclusion from ESR studies for monomeric species.[39] Since the d_{xy} orbital is not expected to interact as strongly as the $d_{x^2-y^2}$ with the porphyrin radical, it might be expected that the ferromagnetic interaction would not be as strong as that seen in $[Cu(TMP•)]^+$. This would lead to magnetic susceptibility data indicatng that the $S = 0$ state could be thermally populated at room temperature, i.e., a triplet–singlet splitting of a few hundred wavenumbers.

The experimental data for [VO(TPP•)][$SbCl_6$], the only vanadylporphyrin radical complex that we have been able to isolate in analytically pure form, are displayed in Figure 7. The significant paramagnetism at room temperature (2.24 μ_B) requires that the $S = 1$ state is readily accessible. However, without a high-temperature limit we cannot tell whether it is depressed from the pure $S = 1$ value (2.83 μ_B) by intermolecular antiferromagnetic coupling or by virtue of a nearby $S = 0$ state within an isolated monomer. The latter situation would lead to a high-temperature limit of $\mu = 2.45$ μ_B which is a reasonable extrapolation for the data. The rapid dropoff of μ_{eff} with temperature must result from intermolecular antiferromagnetic coupling which, in the absence of an X-ray structure, we assume arises from dimer formation.

Nickel. Since nickel(II) is diamagnetic, the formation of $[Ni(porph•)]^+$ presents a useful base line case for magnetic studies. In theory, the compound should behave like a delocalized organic radical and might be expected to easily aggregate and form diamagnetic dimers. By working with the poorly coordinating anion $SbCl_6^-$ and by using a noncoordinating solvent (dichloromethane), we avoided the possible complication of obtaining the Ni(III)[40] redox isomer. In practice, the poor solution stability of Ni(II) porphyrin π-cation radicals allowed the isolation of pure materials only in the case of [Ni(OEP•)][$SbCl_6$]. This material is diamagnetic over the temperature range 6–300 K, and this suggests effective dimerization in the solid state.

Although analytically pure materials were not obtained with [Ni(TPP•)][$SbCl_6$] and [Ni(TMP•)][$SbCl_6$], IR spectra of impure solids did show strong 1280-cm^{-1} absorptions indicative of π-cation radical species. In the case of the more soluble mesityl derivative an Evans method NMR study gave $\mu_{eff} = 2.0$ μ_B, which is consistent with an $S = {}^1/_2$ free radical ($\mu_{theory} = 1.73$ μ_B) in the solution state.

Cobalt. A cobalt(II) radical cation is an attractive candidate for the present studies because similar to copper(II) and vanadyl,

(38) Eaton, G. R.; Eaton, S. S. *Coord. Chem. Rev.* **1978**, *26*, 207.
(39) Lemtur, A.; Chakravorty, B. K.; Dhar, T. K.; Subramanian, J. *J. Phys. Chem.* **1984**, *88*, 5603.
(40) Dolphin, D.; Niem, T.; Felton, R. H.; Fujita, I. *J. Am. Chem. Soc.* **1975**, *97*, 5288.

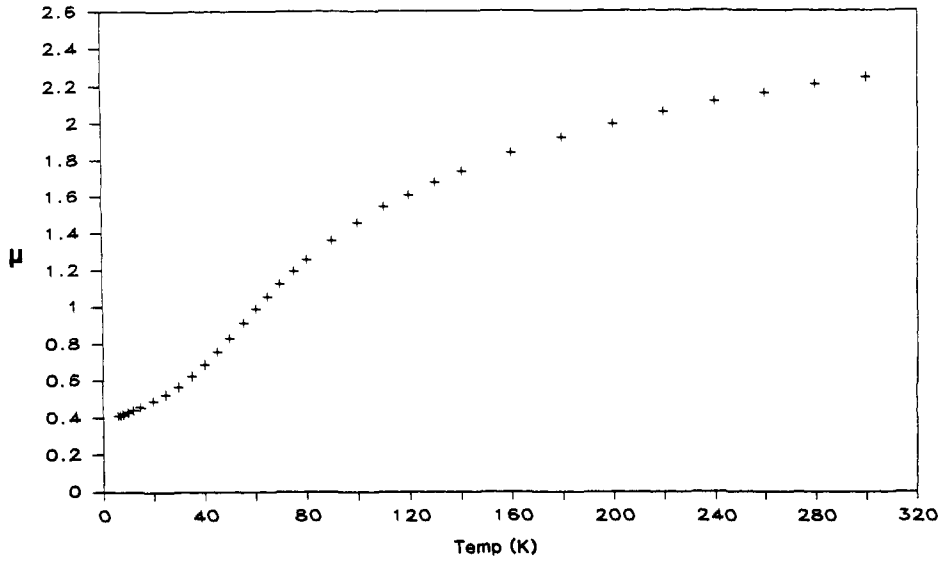

Figure 7. Plot of μ_{eff} vs. temperature for [VO(TPP•)][$SbCl_6$].

the interaction between one unpaired electron on the metal and one on the ligand can be investigated. Cobalt(II) differs by having its unpaired electron in the d_{z^2} orbital, and since the major lobes are not directed at the porphinato N atoms, a smaller magnetic interaction might be expected.

Studies on the oxidation of Co(TPP) have been carried out electrochemically in benzonitrile solution and related dipolar solvents.[14,41] In these studies the single-electron oxidized products were formulated as Co(III) porphyrins based primarily on the intense red-shifted Soret and the typically metalloporphyrin-like UV-vis spectra. The axial coordination of solvent molecules probably stabilizes metal oxidation as opposed to ring oxidation since when we carry out the one-electron oxidation of Co(TPP) in dichloromethane the unmistakable characteristics of π-cation radical formation are observed. There is a fourfold diminution of intensity of the Soret band and a blue-shift from 416 to 398 nm. The α,β region broadens considerably. The IR spectrum of the isolated material shows the diagnostic 1290-cm^{-1} absorption as a strong band. These UV-vis changes are mirrored in the one-electron oxidation of Co(OEP) in dichloromethane, suggesting that a ring-oxidation assignment is preferable to the cobalt(III) formulation it has been given previously.[42] This conclusion is endorsed by very recent spectroscopic work.[43]

For reasons of solubility an entirely reliable measurement of the magnetic susceptibility of [Co(TPP•)][$SbCl_6$] in dichloromethane could not be obtained. The *p*-tolyl analogue, however, yielded an ambient temperature moment of 2.5 μ_B. This is within experimental error of the 2.45 μ_B value expected if there is little (<100 cm^{-1}) interaction between the metal and ligand spins. It shows that the $S = 1$ state is low lying but does not allow the ordering or the separation of states to be fully determined. In the solid state [Co(TPP•)][$SbCl_6$] is diamagnetic, presumably because of both strong intermolecular π–π coupling in a dimer structure and strong intramolecular d–π coupling within a ruffled $[Co(TPP^{\bullet})]^+$ unit.

Iron. Copper, vanadyl, and cobalt provide $S = {}^1/_2$ metal-based spins in $d_{x^2-y^2}$, d_{xy}, and d_{z^2} orbitals, respectively. The remaining possibility arises for an unpaired electron in the d_{xz} (or d_{yz}) orbital. Such a case is provided by low-spin iron(III) in $[Fe(TPP^{\bullet})(1\text{-MeIm})_2]^{2+}$, a species of limited stability that has been prepared in solution at low temperature.[44] Although originally suggested as a case of noninteracting spins (i.e., $S = 1$ and $S = 0$ states equal in energy), we have argued that the magnetic moment and the ^1H NMR data are better interpreted in terms of an $S = 1$ ground state arising from strong ferromagnetic coupling.[2] The spatial disposition of the d_π magnetic orbital on iron is ideal for a strong interaction with the porphyrin π magnetic orbital, and the interaction is ferromagnetic because orthogonality is retained even if the local iron symmetry is lowered to C_{2v}.

Conclusion. The opportunity provided by the present $S = {}^1/_2/S = {}^1/_2$ systems to study spin coupling between a porphyrin π-radical as a function of spin in each of the four symmetry-distinct d orbitals has led to a consistent set of guiding principles for understanding metal–ligand magnetic coupling.

Metalloporphyrin π-radicals show intramolecular *ferro*magnetic coupling when their magnetic orbitals are orthogonal. Orthogonal orbitals will frequently be the result of attaining a planar core structure, something which is greatly assisted by the use of the sterically bulky tetramesitylporphyrin to prevent intermolecular aggregation and accompanying porphyrin core ruffling. The ferromagnetic interaction between the metal and ligand spins is conceptually the same as Hund's rule of maximum multiplicity. It differs only in that the orbitals are not exactly degenerate. The exchange interaction between unpaired electrons, which because of their mutual proximity must "know" of each other's presence but are forbidden by symmetry to overlap, gives rise to the higher multiplicity state. In this sense, the porphyrin HOMO acts like a sixth d orbital. Its symmetry is, afterall, defined from the same origin.

When the metal and ligand orbitals can undergo a symmetry-allowed overlap, as in most nonplanar metalloporphyrin π-radicals, we get *antiferro*magnetic coupling. This is conceptually indistinguishable from bond formation whereby a metal electron and a ligand electron are spin paired in a bonding molecular orbital. The spin state of lower multiplicity is lower in energy. Since, energetically, overlap terms quickly dominate over exchange terms, it is likely that rather little departure from strict orthogonality-producing symmetry is required for antiferromagnetic coupling to dominate over ferromagnetic coupling. It may be possible eventually to manipulate this trade-off of opposing effects to identify and control the type of interaction desired. The variables of particular d orbital occupation, a_{1u} or a_{2u} type of radical, porphyrin symmetry, and lattice symmetry suggest a rational way of approaching this problem.

The potential generality of the theory is attractive, and if no exceptions can be found,[45] metalloporphyrin π-cation radicals may

(41) Walker, F. A.; Beroiz, D.; Kadish, K. M. *J. Am. Chem. Soc.* **1976**, *98*, 3484.
(42) Dolphin, D.; Forman, A.; Borg, D. C.; Fajer, J.; Felton, R. H. *Proc. Natl. Acad. Sci. U.S.A.* **1971**, *68*, 614.
(43) Salehi, A.; Oertling, W. A.; Babcock, G. T.; Chang, C. K. *J. Am. Chem. Soc.* **1986**, *108*, 5630.
(44) Goff, H. M.; Phillippi, M. A. *J. Am. Chem. Soc.* **1983**, *105*, 7567.
(45) We are reinvestigating the [MnCl(TPP•)][$SbCl_6$] system whose reported magnetic data[17,46] differ from those gathered in our laboratories[47] and whose structure unexpectedly is reported to be planar.[17]
(46) Goff, H. M.; Phillippi, M. A.; Boersma, A. D.; Hansen, A. P. *Adv. Chem. Ser.* **1982**, *201*, 357.

provide the most readily accessible and heuristically useful introduction that is presently available for understanding the fundamental concepts of magnetic coupling phenomena.

Acknowledgment. This work was supported by the National Science Foundation (CHE 80 26812, CHE 85 19913 to C.A.R.) and the National Institutes of Health (HL 15627 to W.R.S.). The Squid susceptometer used in this work was purchased with assistance from an NSF Instrumentation Grant (CHE 82 11349).

(47) Erler, B. S. Ph.D. Thesis, University of Southern California, 1985.

Supplementary Material Available: Table IS, anisotropic temperature factors; Table IIS, fixed hydrogen atom positions; Table IIIS, bond distances; Table IVS, bond angles; listings of magnetic susceptibility data for $[Cu(TMP^{\bullet})][SbCl_6]\cdot C_6H_5F$ and $[VO(TPP^{\bullet})][SbCl_6]$ (9 pages); listings (×10) of the observed and calculated structure amplitudes of $[Cu(TPP^{\bullet})][SbCl_6]$ (13 pages). Ordering information is given on any current masthead page.

Crystal Disorder and Triboluminescence: Triethylammonium Tetrakis(dibenzoylmethanato)europate

Linda M. Sweeting*[†] and Arnold L. Rheingold[‡]

Contribution from the Departments of Chemistry, Towson State University, Baltimore, Maryland 21204, and University of Delaware, Newark, Delaware 19716.
Received September 30, 1986

Abstract: Triethylammonium tetrakis(dibenzoylmethanato)europate is found to exist in two crystal modifications, one of which is triboluminescent (**1**). Both forms crystallize in the centrosymmetric monoclinic space group $I2/a$. The non-triboluminescent form (**2**) contains cocrystallized solvent (CH_2Cl_2); the triboluminescent form does not, but it is disordered. **1**: a = 25.431 (4) Å, b = 9.154 (2) Å, c = 27.643 (4) Å, β = 112.20 (1)°, V = 5937 (2) Å^3, Z = 4, R_F = 7.49%. **2**: a = 25.418 (8) Å, b = 17.997 (7) Å, c = 27.253 (8) Å, β = 94.25 (2)°, V = 12432 (6) Å^3, Z = 8, R_F = 5.07%. Crystal forms **1** and **2** have the same fluorescence spectra in the solid state, indicating that the dichloromethane does not quench the triboluminescence by quenching the fluorescence. We conclude that the disorder in **1** provides a means of separating charge during fracture and propose a general theory of triboluminescence dependent on charge separation and dielectric breakdown.

Many crystals emit light upon fracture; this phenomenon, known as triboluminescence,[1] has been studied for centuries[2] but is not well understood. There is substantial evidence that charge separation created during fracture is the immediate precursor of the triboluminescent emission.[3] Crystals of nonfluorescent compounds emit the dinitrogen discharge spectrum as their triboluminescence; crystals of fluorescent compounds emit their fluorescence spectra, often modified and occasionally combined with the dinitrogen discharge spectrum, when they triboluminesce. In those cases where the dinitrogen spectrum is observed, it is probable that charge is separated during stress or fracture and recombination occurs by dielectric breakdown of the atmosphere.[4] The emission of the dinitrogen excited during the breakdown (lightning) excites the fluorescence of the crystal. For fluorescent materials which do not exhibit the dinitrogen spectrum, the process may be the same but with a very low intensity of dinitrogen emission. Alternatively, a fluorescent material may be excited directly, with any dinitrogen emission representing an independent phenomenon; spectroscopic studies have not been able to distinguish these two possibilities.[5]

Since triboluminescence is very common among polar crystals, it has often been claimed[6] that noncentrosymmetric, polar, and therefore piezoelectric crystals are *necessary* for the observation of triboluminescence; such materials would certainly generate opposite charge on opposing faces of cracks perpendicular to the polar axis. Although the evidence for the electrical nature of triboluminescence is quite good, there are many centrosymmetric crystals which are triboluminescent[6] and many noncentrosymmetric crystals which are not.[7] Several materials (e.g., saccharin[8] and zinc sulfide[9]) are triboluminescent because of impurities; however, there is no evidence that triboluminescent materials are generally more or less pure than similar nontriboluminescent materials.

We have been searching for a clear pattern of triboluminescence activity as a function of crystal structure that would permit the construction of a predictive theory of triboluminescence. To this end we have studied triethylammonium tetrakis(dibenzoylmethanato)europate, one of the most brilliantly triboluminescent compounds known.[10] In this paper, we compare a triboluminescent crystal form (**1**) with a nontriboluminescent form containing solvent of crystallization (**2**) and provide evidence for a general theory of triboluminescence.

Experimental Section

Preparation and Characterization. The triethylammonium tetrakis(dibenzoylmethanato)europate was synthesized by the method of Hurt et al.;[10] the crude material was strongly triboluminescent. Purification by recrystallization was accomplished by room temperature evaporation of solvent. Form **1** was obtained by recrystallization from methanol (Fisher reagent): yellow plates, strongly triboluminescent, mp 171-80 °C, IR 1600 cm^{-1} (C=O), solid fluorescence max 614 nm (doublet).

[†] Towson State University.
[‡] University of Delaware.

(1) Also known as fractoluminescence of mechanoluminescence.
(2) Bacon, F. *The Advancement of Learning*; 1605; Book IV, Chapter 3.
(3) Dickinson, J. T.; Brix, L. B.; Jensen, L. C. *J. Phys. Chem.* **1984**, *88*, 1698-1701. Das, J. N.; Chandra, B. P. *Czech. J. Phys.* **1973**, *B23*, 962-965.
(4) Dickinson, J. T.; Jensen, L. C.; Jahan-Latibari, A. *J. Vac. Sci. Technol.* **1984**, *2*, 1112-1116.
(5) Walton, A. J. *Adv. Phys.* **1977**, *26*, 887-948.
(6) Chandra, B. P.; Zink, J. I. *J. Lumin.* **1981**, *23*, 363-372. Chandra, B. P.; Elyas, M.; Shrivastava, K. K.; Verma, R. D. *Solid State Commun.* **1980**, *36*, 931-933.
(7) For example, sucrose and glucose are triboluminescent and fructose and galactose are not. Zink, J. I.; Hardy, G. E.; Sutton, J. E. *J. Phys. Chem.* **1976**, *80*, 248-249.
(8) Hardy, G. E.; Kaska, W. C.; Chandra, B. P.; Zink, J. I. *J. Am. Chem. Soc.* **1981**, *103*, 1074-1079.
(9) Thiessen, P. A.; Meyer, K. *Naturwissenschaften* **1970**, *57*, 423-427.
(10) Hurt, C. R.; McAvoy, N.; Bjorklund, S.; Filipescu, N. *Nature (London)* **1966**, *212*, 179-180.

0002-7863/87/1509-2652$01.50/0